Vacuum 207 (2023) 111573

Contents lists available at ScienceDirect

Vacuum

journal homepage: www.elsevier.com/locate/vacuum

Comparison of ionization vacuum gauges close to their low pressure limit

Anke Stöltzel *, Berthold Jenninger

CERN, Geneva, Switzerland

ARTICLE INFO

Keywords:
Ionization gauge
Helmer
XHV
UHV
Gauge pumping
Gauge outgassing

ABSTRACT

Parts of CERN's accelerator complex and experiments, especially in the antimatter field, require a vacuum in the 10^{-12} mbar range or better. Thus gauges are needed to reliably measure XHV during experimental operation and in order to study the vacuum science needed for those experiments. We therefore built a setup to reach $1 \cdot 10^{-13}$ mbar in order to simultaneously compare different hot cathode ionization gauges with the ability to measure high UHV and XHV close to their lower pressure limit: Barion extended, Extractor IE514, a modulated Bayard–Alpert gauge and two Improved Helmer gauges. All gauges but the Extractor behave similarly with respect to small pressure variations around the limit pressure, while the Extractor seems to overestimate high UHV hydrogen pressure. We show how gauge operation determines our ultimate achievable pressure due to outgassing, which was comparable for all gauges and in the order of $Q \sim 10^{-10}$ mbar l s^{-1}. Further we show the disturbances caused in the static system due to gauge pumping (visible only as electronic pumping), and report some of the possible difficulties and origins of noise when measuring pressures in the XHV range, including the thermoelectric effect.

1. Introduction

UHV measurements today are mostly carried out by ionization vacuum gauges. There are different types of ionization gauges (IG): cross field gauges (also called cold cathode gauges), which generate a gas discharge between two electrodes, and emitting cathode ionization gauges, which have a continuous and controlled electron emission. The signal in all IG is the resulting ion current, which is proportional to the gas density and thus the pressure. Emitting cathode ionization gauges are mostly hot cathode ionization gauges (HCIG), in which a hot filament serves as the electron source, while cold field emitters are also possible but not commercialized [1].

In some experiments, especially antimatter experiments, and in parts of CERN's accelerator complex like in ELENA (Extra Low ENergy Antiprotons) pressures in the 10^{-12} mbar range or lower are required for operation and therefore need to be measured reliably. Also in vacuum science itself XHV measurements are necessary, as for example for adsorption isotherm measurements at lower coverages than available in the literature today.

The lower pressure limit of XHV gauges is composed of many different effects, including the X-ray effect, electron-stimulated desorption (ESD) of ions, ESD of neutrals, thermal outgassing, and various noise sources. Many of these effects are mitigated in current XHV gauges, but a non-zero residual still remains [1–11].

The purpose of this paper is to assess the status quo of the XHV gauges available to us. We conducted a comparative study with several HCIGs close to their lower pressure limit, which gave us the opportunity to directly compare their different behavior, limitations and influence on a vacuum setup.

2. Characteristics of the gauges studied

We tested four different types of HCIG with lower measurement range limits in the XHV range: the commercial gauges "Barion extended" and "Extractor" IE514 and the CERN specific gauges "modulated Bayard–Alpert" and two "Improved Helmer" gauges, which were manufactured during the of 1970's decade and recently. In the following, the pressure reading of a gauge in nitrogen equivalent is defined as

$$p = \frac{I_c}{I_e \cdot S}, \tag{1}$$

with I_c the ion collector current, I_e the electron emission current and S the sensitivity (in N_2 equivalent) determined in a separate measurement. A summarizing table (Table 1) shows the gauge parameters relevant for the following measurements.

Barion extended. This commercial Bayard–Alpert (BA) gauge by VACOM GmbH has a sensitivity for N_2 of $\sim 25\,\text{mbar}^{-1}$. It has a reduced lower pressure limit of about $5 \cdot 10^{-12}$ mbar compared to conventional BA gauges, whose limit typically is around $3 \cdot 10^{-11}$ mbar [12]. It is mainly

* Corresponding author.
E-mail address: anke.stoeltzel@cern.ch (A. Stöltzel).

https://doi.org/10.1016/j.vacuum.2022.111573
Received 7 January 2022; Received in revised form 14 June 2022; Accepted 3 October 2022
Available online 8 October 2022

achieved by balancing the direct and inverse X-ray effects by design. This means that the direct X-ray effect (i.e., X-rays generated by the impact of electrons on the grid knock electrons out of the ion collector) is largely compensated for by the inverse effect, in which the X-rays generate photoelectrons on the outer walls, which reach the collector. Even though the pressure limit is not as low as for the following gauges, the Barion is nevertheless very interesting for various applications at CERN as it covers the entire range from $5 \cdot 10^{-12}$ mbar to $1 \cdot 10^{-2}$ mbar.

Extractor IE514. This commercial gauge originally developed by Leybold extracts the ions from within the grid and focuses them by a reflector electrode onto a collector pin, which is shielded from X-rays created at the grid. Thus, it achieves a residual pressure of $\sim 2 \cdot 10^{-12}$ mbar. While it has a rather low average sensitivity of $\sim 6\,\text{mbar}^{-1}$, it is compact and relatively robustly built compared to the other HCIG studied.

Following a procedure proposed by Watanabe [13], one can determine the residual pressure caused by X-rays by varying the bias on the reflector electrode with external power supplies and comparing the respective ion current to the residual current when the emission is switched off. Beyond a threshold of reflector voltage of about +350 V, no more ions can reach the collector. In contrast, the electron trajectories around the grid remain unperturbed by the change in reflector bias, due to the shielding provided by grounded aperture. Also the residual current due to X-rays is approximately of the same magnitude in this configuration as at nominal potential (~ 200 V). This is, because the photoelectron current from the collector to the reflector is already saturated at nominal potential and does not increase any further going to higher potentials [13]. If this X-ray induced current is subtracted from the total measured ion current, a lower pressure limit in the low 10^{-13} mbar range can be achieved.

Modulated Bayard–Alpert gauge (mBA). In the 1970s a BA type gauge has been developed for the Intersecting Storage Rings (ISR) as pressures lower than 10^{-11} mbar had to be measured reliably [14]. It is nowadays a most widespread gauge at CERN with over 1000 gauges manufactured. For modulation, it has two modulator rods near the grid so that the residual, X-ray induced current can be determined by switching the rods from grid potential in normal mode to ground potential in modulation mode. Both times the current is measured at the collector and called I_c^{norm} and I_c^{mod} respectively. Presuming the residual current itself is not modulated but only the actual ion current [15], the residual current can be calculated via

$$I_{\text{res}} = I_c^{\text{norm}} - (I_c^{\text{norm}} - I_c^{\text{mod}})/k\,, \tag{2}$$

with the modulation factor k determined at a higher pressure, where I_{res} is negligible and therefore

$$k = 1 - \left.\frac{I_c^{\text{mod}}(p)}{I_c^{\text{norm}}(p)}\right|_{p \gg p_{\text{res}}}\,. \tag{3}$$

Its average characteristics are a high sensitivity of $\sim 32\,\text{mbar}^{-1}$, modulation factor 0.86 and residual pressure $\sim 2.4 \cdot 10^{-12}$ mbar [14]. The mBA is usually used with a dedicated controller (Volotek VGC1000) that allows the modulation. When using an external, more stable electrometer, pressures down to the low 10^{-13} mbar range can be measured.

Improved Helmer gauge (IHG). In a gauge of Helmer's principle [16] (see Fig. 1), ions are extracted from the grid and enter a grounded box (a shield from X-rays), where they are deflected by 90° and guided onto a remote collector plate. Photoelectrons created at ground level are repelled by a negatively biased suppressor grid, while photoelectrons or ion stimulated secondary electrons knocked out of the collector are pushed back.

Further improvements to this gauge were made by Benvenuti and Hauer [11], who increased the sensitivity up to $\sim 30\,\text{mbar}^{-1}$ while pushing down the pressure equivalent residual current to lower than $2 \cdot 10^{-14}$ mbar. They used a thoria coated filament instead of pure tungsten and optimized the ion extraction apertures on grid and shielding box. A few gauges of this type were manufactured at CERN at that time.

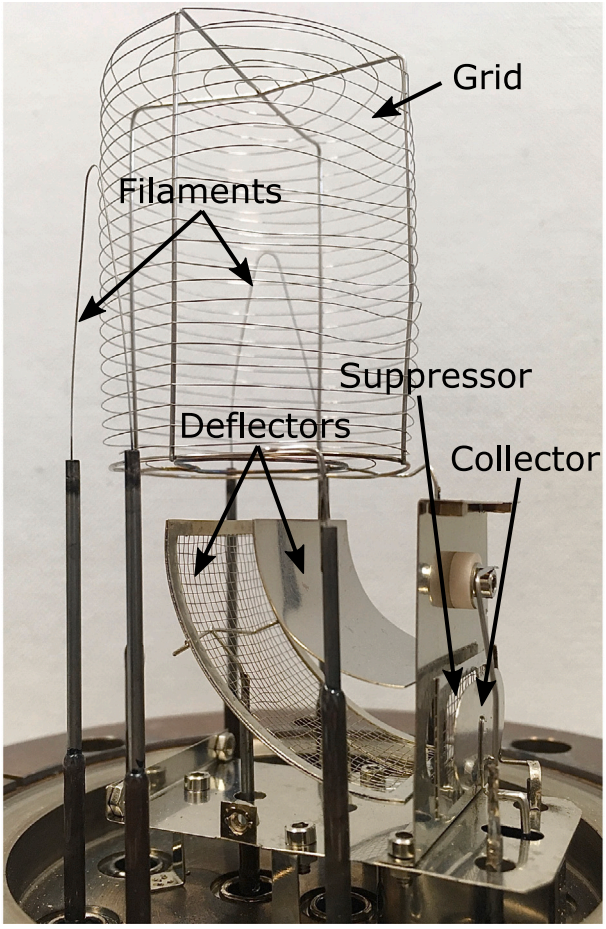

Fig. 1. Improved Helmer gauge, shown without shielding box to see its inner components (lower and upper deflector plate, grounded aperture, suppressor grid and ion collector).

So far the IHG is missing a trustworthy technique to determine the residual current more precisely. Nevertheless, the IHG recorded the lowest pressure ever measured at room temperature $\sim 3 \cdot 10^{-14}$ mbar [17].

As this gauge seems to be a promising candidate to reach the 10^{-14} mbar range and to reliably measure in the 10^{-13} mbar, a manufacturing campaign of four gauges was launched recently. Even with drawings, dating from the 1980's, still available, the manufacturing requires very particular skills including spot welding, handling thin wires and glass feedthroughs, right material choices and correct procedures as for vacuum firing and tooling. Thus we need to compare these new gauges to the old IHG and to other XHV gauges available to us to verify their quality.

3. Experimental setup

Setup design. We built a simple setup that allows to test and compare four gauges simultaneously down to a pressure limit of $\sim 1 \cdot 10^{-13}$ mbar. As schematically shown in Fig. 2, the setup consists of a dome shaped main chamber with four ports for the gauges to be tested, a port for the leak valve to the gas injection system and an elbow at the bottom leading to a all metal angle valve. In total, in the dome and elbow three meter of two-sided, 30 mm wide, St707 Non-Evaporable Getter (NEG) strips are arranged in a way that there is no preferential pumping direction. It is taken care that no port is obstructed. The total pumping speed for hydrogen is estimated to be $3000\,\text{l}\,\text{s}^{-1}$ [18]. The

Table 1
Gauge parameters as they were used in measurements in this work. Pressure limits in parentheses can be achieved after determination and subtraction of the X-ray induced residual current. Note that the Helmer gauges do not operate at potentials optimized for maximum sensitivity when used with the Volotek controller.

	Low pressure limit [mbar]	I_e [mA]	S for N_2 [mbar^{-1}]	Filament	Controller
Barion ext.	$5 \cdot 10^{-12}$	2	25	Yttria coated iridium	MVC-3
Extractor	$2 \cdot 10^{-12}$ (low 10^{-13})	1.6	6	Yttria coated Iridium	CM 52
mBA	$2.4 \cdot 10^{-12}$ (low 10^{-13})	4	30	Tungsten	Volotek VGC1000
IHG 1 IHG 2	$< 2 \cdot 10^{-14}$	1 1	16 15	Thoriated tungsten Tungsten	Volotek with add. lab equipment

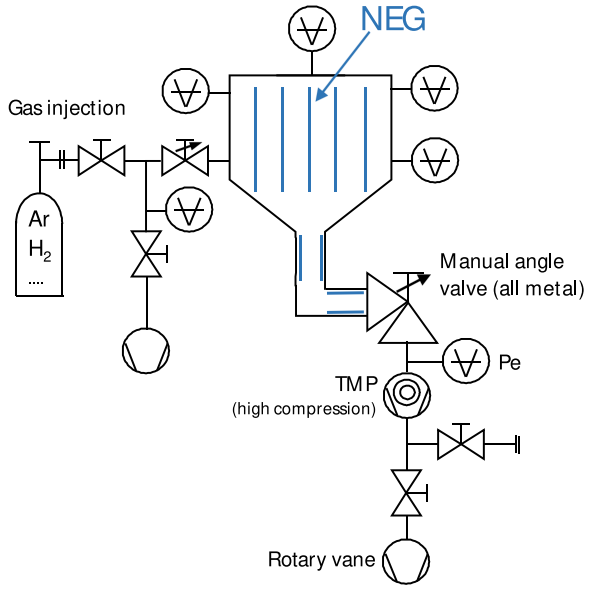

Fig. 2. Schematic setup: Dome filled with NEG stripes, four gauge ports, gas injection system and all metal angle valve to TMP and inverted magnetron (Pe) gauge. Note that the NEG is not actually arranged in columns but chaotically to achieve an isotropic pressure distribution.

specific outgassing rate for H_2 of the dome after vacuum firing and baking is in the low 10^{-14} mbar l s^{-1} cm^{-2} range (at a surface area of the dome of roughly 3000 cm^2) [19]. On the other side of the angle valve is a IKR 70, an inverted magnetron gauge (IMG) by Pfeiffer and a turbo molecular pump (TMP) with a nominal pumping speed of 300 l s^{-1}, backed by a rotary vane pump. The TMP is a H_2 gas load for the setup through back-streaming and outgassing. Gases as CH_4 and noble gases are not pumped by the NEG within the dome but present in the system. This is because of methane outgassing with a specific outgassing rate of about 2 orders of magnitude lower than for hydrogen ($1 \cdot 10^{-16}$ mbar l s^{-1} cm^{-2}) [20], and because argon as a calibration gas is injected into the system up to higher pressures. Argon is therefore implanted in the collector and walls of the gauges, which then are a gas source once back in UHV regime. When balancing the H_2 gas load from the TMP into the dome and its pumping speed for CH_4 and noble gases from the dome, one can find an optimal angle valve position (almost closed with only a small opening remaining), where minimum total pressure within the dome is achieved. With these estimated outgassing rates and pumping speeds, we may expect an ultimate pressure in the low 10^{-14} mbar range, while all gauges remain off. While the exact values may differ, the following measurements prove that the estimates lie at least in the correct order of magnitude.

Homogeneity of pressure distribution within the dome. The gauges and the injection valve are evenly distributed around the main chamber, all with a similar conductance to the NEG and also to the TMP. The effective pumping speed of the TMP at the dome is very small (order of only a few liter per second with an almost closed angle valve), especially in comparison to the NEG's pumping speed of 30001 s^{-1} for hydrogen. We first checked the pressure distribution via step-wise argon injections, which is not pumped by NEG and thus a similar response from all gauges is expected. We found a maximum spread in the pressure readings from the 10^{-12} mbar range to $\sim 1 \cdot 10^{-7}$ mbar of the mBA, Helmer, Extractor and Barion gauges of ±15%. This spread lies within the uncertainties of the gauges' sensitivity. In a second step, the same is repeated with hydrogen injections. Hydrogen is strongly pumped by the NEG and so the homogeneity relies on a small enough sticking factor. Otherwise, if the sticking factor was high, gas from a local source (e.g. a gauge, or in this test the injection port) would be pumped close to the source, increasing the pressure locally, but not reaching all gauges to the same extent. The gauges would record a pressure change depending on their position in the setup. But only a maximum spread of ±10% was observed. This lies as well within the gauges' uncertainty and thus also the H_2 pressure distribution within the dome is sufficiently homogeneous for our purposes.

During hydrogen injections lower than 10^{-10} mbar we observed a drift of the extractor gauge and a higher pressure reading than of the other three gauges (see Fig. 3). This phenomenon was not visible under argon injections or higher H_2 pressures and will be discussed further in the next section.

4. Results of direct comparison

All pressure values presented in the following measurements are in N_2 equivalent and either given as pure pressure reading, averaged over a moving time window or corrected for the different residual pressures as indicated in the figure's captions.

Performance of the Improved Helmer gauges. The newly manufactured Improved Helmer gauges behave comparable to the old IHG by Benvenuti [11]. Their signal stability seems to allow measurements in the 10^{-14} mbar range, while an actual measurement in this range remains open due to the pressure limit of our current setup. There is no dedicated controller for the IHG. For the application in an accelerator we therefore use the conventional mBA gauge controller at CERN. As the mBA does not have a deflector nor suppressor electrode, two additional, external laboratory power supplies are needed. This has the advantage that we profit from the reliable emission control and collector reading, and allowing easy integration into our data acquisition infrastructure. The disadvantage is that the voltages for the filament bias and grid are fixed, so that we can only achieve sensitivities of ~ 15 mbar^{-1}. When we control the IHG with all single power supplies for each electrode and optimize the potentials, a maximum sensitivity of 35 mbar^{-1} at an emission current of 1.7 mA was reached. This sensitivity was determined with the mBA as pressure reference and at a raised pressure within the setup of 10^{-8} mbar (argon injection).

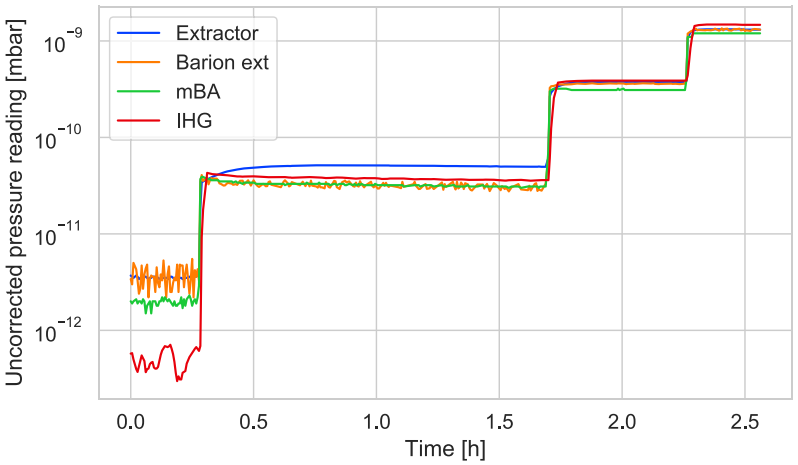

Fig. 3. H_2 injections shortly after bakeout from base pressure to 10^{-9} mbar range. Pressure readings not corrected for their residual and given in N_2 equivalent. Extractor gauge drifts and measures a higher pressure in H_2 atmospheres below 10^{-10} mbar than the other gauges.

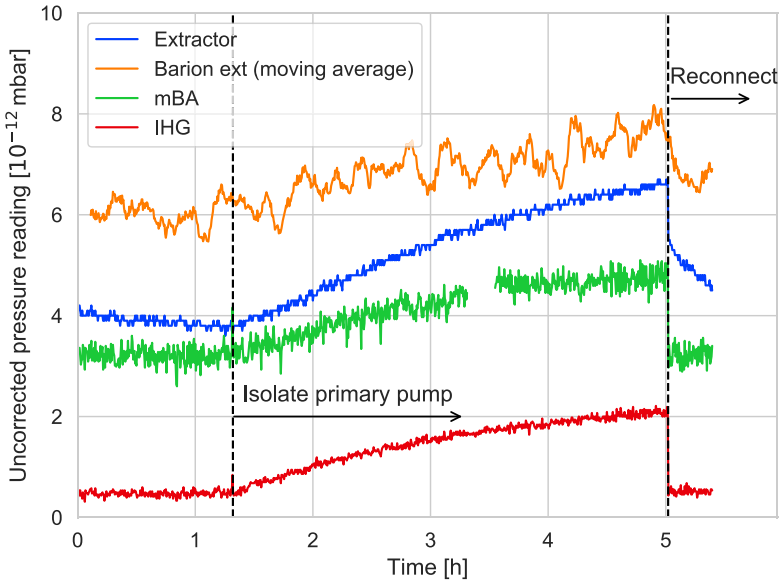

Fig. 4. Gauge's reaction to slow and fast pressure variations by isolating and reconnecting the primary pump. Pressure readings not corrected for their residual and given in N_2 equivalent, Barion averaged over 5 min intervals. Extractor overestimates high UHV H_2 pressures.

Gauge reactions to small H_2 pressure variations. By closing the valve to the rotary vane pump, we found a way to induce small pressure variations in the order of $1 \cdot 10^{-12}$ mbar. The closure of the valve results in a slow pressure rise caused increasing H_2 accumulation downstream of the TMP and the small compression ratio of the TMP for H_2. On opening the valve again a sharp pressure drop is achieved. We show in Fig. 4 how mBA, IHG and Barion rise slowly by the same amount ($\Delta p_{\text{slow}} = 1.6 \cdot 10^{-12}$ mbar), while the Extractor alone rises by $\Delta p_{\text{slow, Extr.}} = 3 \cdot 10^{-12}$ mbar and as before seems to overestimate high UHV H_2 pressures, here about by a factor of 2. Note, that the absolute pressures indicated are not corrected for the different residual pressures but the uncorrected gauge readings. On the fast pressure drop, Helmer and mBA instantaneously recover back to their baseline, while the Extractor also reacts fast but only drops by $\Delta p_{\text{fast, Extr.}} = 1 \cdot 10^{-12}$ mbar and then only slowly recovers. With the Barion gauge a fast pressure drop in this range cannot be observed due to the applied moving average (window size 5 min, 20 values), necessary because of the strong noise near its pressure limit.

Cycling Barion extended. As the specified upper measurement limit of the Barion extended exceeds all the other gauges, we used the inverted magnetron gauge (IMG) separated from the dome by the angle valve (see Fig. 2) as the comparison gauge for a linearity check. We adjusted the ratio between the pressure in the dome and in the region behind the valve by keeping the valve in a nearly closed position. A ratio of about 120 reduces the pressure behind the valve to the measurable and still linear range of the IMG in argon atmospheres, where we accepted a relative error of up to 10 %. Within the pressure range $1 \cdot 10^{-7}$ to $6 \cdot 10^{-3}$ mbar at the Barion gauge, and thus $8 \cdot 10^{-10}$ to $5 \cdot 10^{-5}$ mbar at the IMG, we found the deviations from linearity to be within ±15 %. Closer to the lower pressure limit of the IMG ($\sim 1 \cdot 10^{-10}$ mbar), these deviation grew up to 30 %, but can be attributed rather to the absolute uncertainties of the IMG near its lower limit than to the Barion gauge.

Remarkable also is the fast recovery after stopped injections. The Barion went from $1 \cdot 10^{-2}$ mbar back to base pressure in the 10^{-12} mbar range in about 2 h, while the IMG gauge needed to be switched off to recover from pollution. Furthermore, its pressure range exceeds the IMG on the lower and higher pressure end.

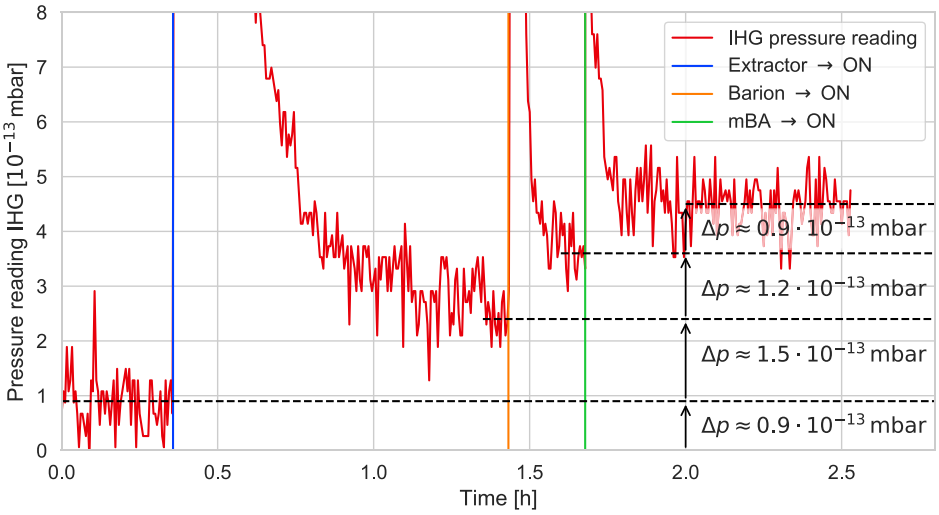

Fig. 5. Outgassing due to filament operation at limit pressure. IHG indicating the total pressure (in N_2 equivalent) when igniting the filaments of the other gauges. Gauges have comparable outgassing rates in the order of $\sim 10^{-10}$ mbar l s^{-1} (two weeks after bakeout).

Gauge outgassing due to filament operation at limit pressure. After about two weeks of pumping after bakeout, the setup reached the pressure $1 \cdot 10^{-13}$ mbar with only the Helmer gauge operating. When igniting the filaments the other gauges one after the other, while the controllers were running and the voltages already set, we can clearly demonstrate that the pressure in our system is dominated by gauge outgassing. If no gauge was operating, the pressure would indeed be in the low 10^{-14} mbar range.

Once the first pressure spike subsides, the pressure rise due to each gauge, as indicated by the IHG, is in the order of $1 \cdot 10^{-13}$ mbar (Fig. 5). Further, we see a longer stabilization time after igniting the filament of the Extractor than as observed for the other two gauges.

For a vacuum system in equilibrium the pressure is

$$p = Q/q_V \,, \tag{4}$$

with the total gas load Q and the effective pumping speed or volume flow rate q_V. On turning on the filament of a gauge, both the pumping speed and the outgassing rate change and the differential pressure change dp is

$$dp = -\frac{Q}{{q_V}^2} dq_V + \frac{1}{q_V} dQ \,. \tag{5}$$

In this measurement, the change in pumping speed due to operation of one gauge more is negligible for all gases present in the system as the NEG for H_2 and the TMP for CH_4 and noble gases are much bigger than the gauges pumping speed:

$$dp \approx \frac{1}{q_V} dQ \;\rightarrow dQ \approx dp \cdot q_V \,. \tag{6}$$

Given that the gauge outgassing is hydrogen dominated, we can estimate with the NEG's pumping speed of $q_V \approx 3000\,\mathrm{l\,s^{-1}}$ and $dp \approx 10^{-13}$ mbar the outgassing rate due to filament operation, not total outgassing rate, per gauge to be in the order of $dQ \approx 10^{-10}$ mbar l s^{-1} two weeks after bakeout. These approximate values are consistent with other measurements as performed in [21–23].

Gauge pumping. The following measurement was performed with a varied gauge configuration, where the Barion gauge was replaced with a new IHG. We show the effect of gauge pumping in the static setup, i.e the angle valve is closed and the TMP isolated. In this configuration, the partial pressures of gases pumped by the NEG are only little affected. In the case of CH_4 and noble gases, the only remaining pumps in the system are the gauges themselves with the properties given in Table 1.

We observe that we can keep a pressure in the range of $6 \cdot 10^{-13}$ mbar only by gauge pumping for CH_4 and noble gases, while the NEG keeps the H_2 pressure close to the prior value.

We consider two different pumping mechanisms in hot filament ionization gauges:

- chemical pumping, the dissociation of molecules on the hot filament and adsorption of the reactive fragments on the walls, electrodes or in our case also the NEG and
- ionic pumping, the collection of ionized molecules on the collector or the walls.

CH_4 will be mainly pumped after dissociation, while ionic pumping affects both CH_4 and noble gases (mainly argon in our setup).

After a stabilization time in section 1 of Fig. 6 we get a new equilibrium pressure of the closed setup p_0 and can write

$$V \left.\frac{dp(t)}{dt}\right|_{t=10\,\mathrm{h}} = 0 = Q_0 - q_{V_0} p_0 \,. \tag{7}$$

Let us now consider the event in section 2 of Fig. 6, switching off the emission of Helmer 2 at $t = 10$ h, and set this moment as the new time zero $t_0 = 0$. The pressure observed by the Extractor rises according to the equation [24]

$$V \frac{dp(t)}{dt} = Q(t) - q_V p(t) \,. \tag{8}$$

For simplification, we assume $Q(t)$ to be constant, i.e. $Q(t) = Q_0$, even though not exactly correct, as the system will cool down slowly after emission on the gauge has been stopped. But as we have seen from our outgassing measurement, the pressure change in the system when switching off the emission of a Helmer gauge is small ($< 0.9 \cdot 10^{-13}$ mbar) with respect to the new base pressure of $p_0 \approx 8 \cdot 10^{-13}$ mbar. The solution of Eq. (8) is

$$p(t) = \frac{Q_0}{q_V} + \left(p_0 - \frac{Q_0}{q_V}\right) e^{-\frac{t}{\tau}} \,, \text{ where } \tau = \frac{V}{q_V} \,. \tag{9}$$

This can be fitted to our data as is shown in Fig. 7. The derivative of Eq. (8) in $t_0 = 0$ is

$$\frac{dp(0)}{dt} = -\frac{q_V}{V}\left(p_0 - \frac{Q_0}{q_V}\right) \,. \tag{10}$$

With the fit parameters and the propagation of their uncertainties we can determine this derivative in the moment of switching off the emission from the filament of Helmer 2 to $(9.33 \pm 0.87) \cdot 10^{-13}$ mbar h^{-1} .

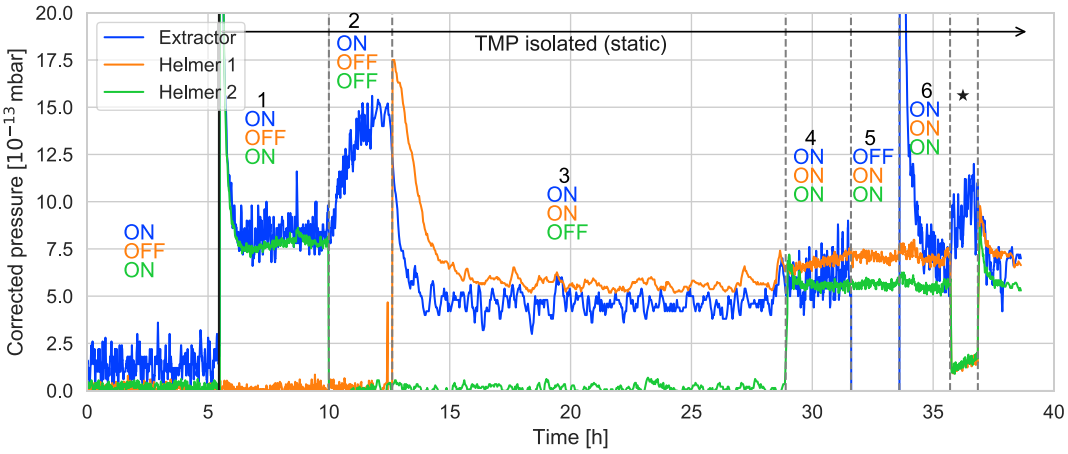

Fig. 6. Effect of gauge pumping in static system. Pressure readings are corrected for residual pressure and offsets (and given in N_2 equivalent). From $t \approx 5\,\mathrm{h}$ the system is isolated and the filaments of different gauges are switched on and off according to the labels in each sections of this figure. ⋆-section: Changing the emission current on both Helmer gauges from 1 mA to 0.2 mA and back. Pressure reading on Helmer gauges reduced during this time as sensitivity remained calibrated for 1 mA.

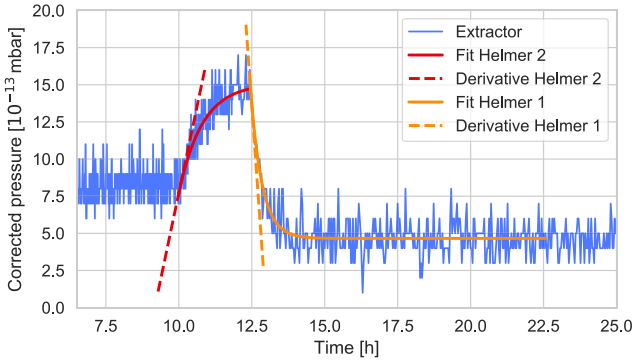

Fig. 7. Zoom into the transition of section 1 to 2 and 2 to 3 of Fig. 6. Fitting pressure evolution formula to data and its derivative in the moment of toggling a gauge.

The volume of the setup is $V = (6 \pm 1)\,\mathrm{l}$ and so the pumping speed of Helmer 2 can be estimated to

$$q_{V_{Helmer\,2}} = \frac{V \frac{dp(0)}{dt}}{p_0} = (2.06 \pm 0.48) \cdot 10^{-3}\,\mathrm{l\,s^{-1}}\,, \quad \text{at } p \approx 7.5 \cdot 10^{-13}\,\mathrm{mbar}\,. \tag{11}$$

Applying the same procedure to the ignition of the filament of Helmer 1 in section 2 of Fig. 6, we get a pumping speed of

$$q_{V_{Helmer\,1}} = (2.97 \pm 0.80) \cdot 10^{-3}\,\mathrm{l\,s^{-1}}\,, \text{ at } p \approx 7.5 \cdot 10^{-13}\,\mathrm{mbar}\,. \tag{12}$$

These values lie in the lower range of published gauge pumping values [24] and in the order of the ionic gauge pumping, as can be estimated in the following way. From Eq. (1) we get

$$I_c = I_e \cdot S \cdot p = \frac{dN_{\mathrm{Ions}}}{dt} \cdot e \cdot S \cdot p\,, \tag{13}$$

and with the ideal gas law the ionic pumping speed estimate is

$$q_{V_{\mathrm{ionic}}} = \frac{I_e}{e} \cdot S \cdot k_B \cdot T\,, \tag{14}$$

with the gauge's sensitivity S, the emission current I_e, the Boltzmann constant k_B and the temperature T. For our gauges we get

$$\begin{aligned} q_{V_{\mathrm{ionic,\,IHG1}}} &= 4.0 \cdot 10^{-3}\,\mathrm{l\,s^{-1}}\,, \\ q_{V_{\mathrm{ionic,\,IHG2}}} &= 3.8 \cdot 10^{-3}\,\mathrm{l\,s^{-1}}\,, \\ q_{V_{\mathrm{ionic,\,Extr.}}} &= 2.4 \cdot 10^{-3}\,\mathrm{l\,s^{-1}}\,. \end{aligned} \tag{15}$$

These values do not account for ions created outside of the grid and pumped at the walls, which would increase the estimated pumping speeds. Further it assumes that all ions collected are actually implanted in the collector and not neutralized, which is actually the far more common mechanism and reduces the estimated number. Overall, these values should give an order of magnitude of the ionic pumping speed.

So it seems that we only see the ionic part of gauge pumping and not the chemical part, which is supported by the observations in the ⋆-section of Fig. 6: The pumping speed goes down with the emission current, while if we observed chemical pumping, the filaments should be still hot enough for efficient dissociation also at a reduced emission current.

The situation seems to be different, when we change from two to three gauges operating (instead of from one to two). In section 4 of Fig. 6, the filament of Helmer 2 is ignited, so that all three gauges are operating.

We do not see any gauge pumping effect but, on the contrary, even a slow pressure rise. Switching off the emission of the Extractor gauge in section 5 also does not give a pressure rise and switching it back on in section 6 does not result in a pressure drop. Generally, igniting the filament of a gauge decreases the methane and argon partial pressures due to gauge pumping, but the hydrogen partial pressure increases due to thermal outgassing ($\Delta p \approx 1 \cdot 10^{-13}\,\mathrm{mbar}$ per gauge). As we only monitor the total pressure, we argue that in the case of two gauges operating, the hydrogen partial pressure is so dominant that the drop in methane and noble gases' partial pressure on turning on a third gauge is no longer visible as these partial pressures are already by two gauges pumped to lower values than the resolvable with the gauges.

This argument is also supported by calculations. If we assume a typical specific methane outgassing of $10^{-16}\,\mathrm{mbar\,l\,s^{-1}\,cm^{-2}}$ (two orders of magnitude less than hydrogen outgassing) [20], and that every molecule impinging on the surface of the filament will also be dissociated and pumped, we see that the methane partial pressure would remain under $1 \cdot 10^{-13}\,\mathrm{mbar}$ in all gauge configurations and therefore for below our measurement background. Furthermore, it stabilizes within seconds on toggling a gauge and not within the order of 1 h as observed. This suggests that the decrease in methane partial pressure, when changing from one to two gauges operating, is not visible in the total pressure of our measurement and that the observed pumping mainly is ionic pumping of argon.

Taking the measured pumping speeds as purely ionic pumping of argon, we can calculate the necessary average specific argon outgassing rate to reproduce the measurement. We obtain $10^{-19}\,\mathrm{mbar\,l\,s^{-1}\,cm^{-2}}$. Note that this does not have to be uniformly outgassed by the walls, but

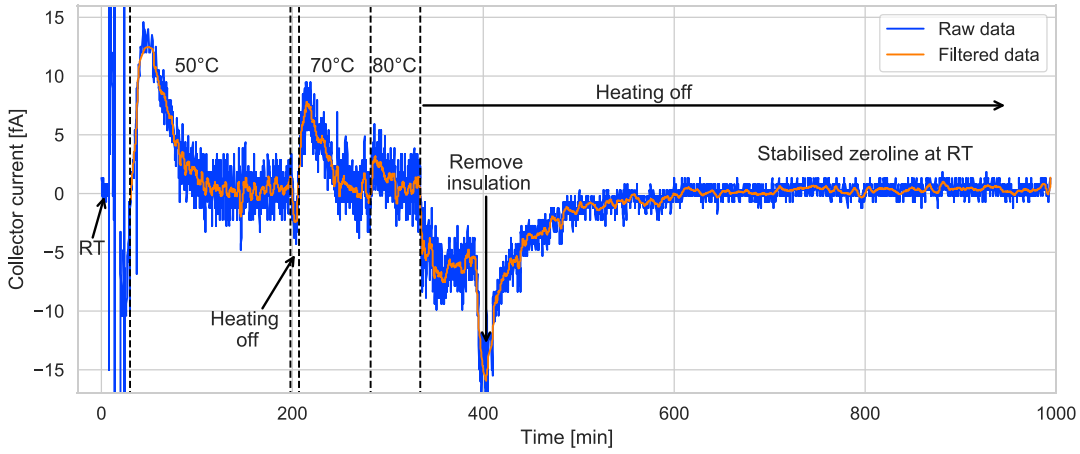

Fig. 8. Charge diffusion due to temperature change. Measured as current on the collector pin of the switched off IHG, i.e. no voltages, no emission. Regular bake-out equipment used for heating.

originates more likely from welds or the gauges. For it must be borne in mind that the gauges were exposed to high argon pressures during previous measurements, which can also reduce the gauge pumping speed further as previously adsorbed argon desorbs and constitutes an additional gas load.

5. Encountered difficulties when measuring pressures in the XHV range

When measuring a pressure of $1 \cdot 10^{-13}$ mbar with an ionization gauge at 1 mA emission current and a high sensitivity of $30\,\mathrm{mbar}^{-1}$, one has to reliably detect an ion current as low as $3 \cdot 10^{-15}$ A. This is not an easy task and one has to carefully shield the collector pin, use a shielded cable and an electrometer with a high amplification and ideally a low pass filter. For our IHG we currently use the current amplifier DDPCA-300 from FEMTO, which has a gain up to $10^{13}\,\mathrm{V\,A}^{-1}$ and a peak-to-peak noise (in the 0.1 Hz low pass filter setting) of 0.4 fA according to its technical specification, which we could also verify when isolating the device. But it has an input current bias of up to 30 fA, which needs to be accounted for and which also drifts, especially due to temperature change up to a factor 2 per 10 °C.

The current amplifier is not the only source of noise. Power supplies connected to the gauge's electrodes couple in noise onto the collector, especially critically being the suppressor. Together with the collector plate it forms a capacitor and thus high frequency noise is easily transmitted. Furthermore, weather conditions (affecting the humidity and ion concentration in the ambient air), temperature and air convection (caused by air conditioning or even opening the laboratory's door) can greatly influence the measurement.

It is hard to give a noise level characterizing each gauge, as it is not only determined by the gauge itself. The usage of stable, low noise power supplies and a careful treatment of the collector pin, i.e. using a shielded cable and a good electrometer with a low pass filter, can achieve lower noise levels for all gauges compared to results obtained with the standard controller. Therefore, when optimizing for low noise, we kept the gauge controller for emission control and voltage supply, but used the FEMTO electrometer for the collector current. This special treatment is possible for the IHG, mBA and also of the Extractor, as their collector pins are accessible individually and can be connected to a shielded BNC-cable, while this is not true for the Barion gauge.

Another effect to consider is the thermoelectric or Seebeck effect: A temperature gradient, somewhere along the chain of collector, feedthroughs and wires to the ammeter, causes a net diffusion of electrons within the material, until the resulting voltage across it equals out the difference in thermodynamic chemical potential. This temporary current can be measured at the electrometer and can lead to a false pressure interpretation when temperature changes occur. In order to demonstrate this effect, we used the bake-out equipment on the flange of the IHG to cause a temperature increase at the gauge through radiation, while it is fully switched off, i.e. no electron emission or filament heating, and no voltages applied to any of the electrodes. As shown in Fig. 8, we first heat from room temperature (RT ~ 20 °C) to 50 °C, switching the heating briefly off and then back on up to 70 °C and 80 °C, before it cools down back to RT. We observe a current peak depending on ΔT as high as $0.5\,\mathrm{fA\,K}^{-1}$, which corresponds to a pressure reading of $2.5 \cdot 10^{-14}\,\mathrm{mbar\,K}^{-1}$ (exemplary for $I_e = 1$ mA and $S = 20\,\mathrm{mbar}^{-1}$). At each temperature, the current on the collector pin relaxes back to the same zero-line as at RT but at an increased noise level. This is due to a possibly higher temperature at the ammeter, increased convection and a pulsed, non-stable heating on the bake-out collar regulating the temperature.

6. Summary and outlook

We built a simple setup to reach $1 \cdot 10^{-13}$ mbar, which allowed us to compare four different gauges simultaneously in this pressure range. The two CERN gauges, mBA and IHG, behave similarly with respect to small pressure variations around the limit pressure, while we have seen the extractor deviating from them in measurements at high UHV hydrogen pressure. We showed how gauge operation determines our ultimate achievable pressure due to outgassing, which was comparable for all gauges and in the order of $Q \sim 10^{-10}\,\mathrm{mbar\,l\,s}^{-1}$. Further we showed the disturbances caused in the static system due to gauge pumping and reported some of the possible difficulties and origins of noise when measuring pressures in the XHV range, including the thermoelectric effect.

We are currently working on alternative gauge concepts with higher sensitivities and thus higher signal to noise ratios as to make a measurement in the XHV range easier. Moreover, all current XHV gauges have hot filaments, which makes it impossible to use them at cryogenic temperatures, especially at liquid helium temperatures, where many experiments operate and where even the heat load of a thoriated filament with a few Watt is unacceptable. So another focus lies on the design of a gauge, which could be installed in a cryogenic system and measure locally at the point of interest without the need for a cold-warm transition with all the associated uncertainties.

CRediT authorship contribution statement

Anke Stöltzel: Conceptualization, Data curation, Formal analysis, Investigation, Methodology, Visualization, Writing – original draft, Writing – review & editing. **Berthold Jenninger:** Writing – review & editing, Supervision, Data curation, Conceptualization.

Declaration of competing interest

The authors declare that they have no known competing financial interests or personal relationships that could have appeared to influence the work reported in this paper.

Data availability

Data will be made available on request.

Acknowledgments

We would like to acknowledge the work of Philippe Lancon and Christian Duclos, who manufactured two new Improved Helmer gauges each and further the work of Nikolaos Chatzigeorgiou, who developed a IHG prototype controller used in parts of our measurements.

References

[1] K. Jousten, F. Boineau, N. Bundaleski, C. Illgen, J. Setina, O.M. Teodoro, M. Vicar, M. Wüest, A review on hot cathode ionisation gauges with focus on a suitable design for measurement accuracy and stability, Vacuum 179 (2020) 109545.
[2] P.A. Redhead, Extreme high vacuum, 1999.
[3] P.A. Redhead, Ultrahigh vacuum pressure measurements: Limiting processes, J. Vac. Sci. Technol. 5 (5) (1987) 3215–3223.
[4] P.A. Redhead, New hot-filament ionization gauge with low residual current, J. Vac. Sci. Technol. 3 (4) (1966) 173–180.
[5] P.A. Redhead, Measurement of residual currents in ionization gauges and residual gas analyzers, J. Vac. Sci. Technol. 10 (4) (1992) 2665–2673.
[6] F. Watanabe, "Total pressure measurement down to 10-12 Pa without electron stimulated desorption ion errors", J. Vac. Sci. Technol. 11 (4) (1993) 1620–1626.
[7] F. Watanabe, My never-ending story towards XHV pressure measurements, Vacuum 53 (1) (1999) 151–157.
[8] F. Watanabe, Dominance of electron-stimulated desorption neutral species in ultra-high vacuum pressure measurements, Vacuum 52 (3) (1999) 333–338.
[9] J. Helmer, History and development of the UHV Helmer gauge as an analytic instrument, Vacuum 51 (1) (1998) 7–10.
[10] C. Benvenuti, M. Hauer, Low pressure limit of the bayard-alpert gauge, Nucl. Instrum. Methods 140 (3) (1977) 453–460.
[11] C. Benvenuti, M. Hauer, Improved helmer gauge for measuring pressures down to 10^{-12} Pascal, Tech. rep., CM-P00064854, 1980.
[12] N. von Freyhold, M. Walter, H. Wunderlich, J. Iwicki, M. Flämmich, U. Bergner, Innovativer Bayard-Alpert Sensor mit ausgetrickster Röntgengrenze, Vakuum in Forschung Und Praxis 24 (5) (2012) 12–16.
[13] F. Watanabe, New x-ray limit measurements for extractor gauges, J. Vac. Sci. Technol. Vacuum, Surfaces, and Films 9 (5) (1991) 2744–2746.
[14] C. Benvenuti, J.M. Laurent, F. Scalambrin, Pressure measurements for the ISR at CERN, Tech. rep., CERN, 1977.
[15] P. Redhead, Modulation of Bayard-Alpert gauges, J. Vac. Sci. Technol. 4 (2) (1967) 57–62.
[16] J. Helmer, W. Hayward, Ion gauge for vacuum pressure measurements below 1×10^{-10} Torr, Rev. Sci. Instrum. 37 (12) (1966) 1652–1654.
[17] C. Benvenuti, P. Chiggiato, Obtention of pressures in the 10^{-14} torr range by means of a Zr-V-Fe non evaporable getter, Vacuum 44 (5–7) (1993) 511–513.
[18] C. Benvenuti, P. Chiggiato, Pumping characteristics of the St707 nonevaporable getter (Zr 70 V 24.6-Fe 5.4 wt%), J. Vac. Sci. Technol. 14 (6) (1996) 3278–3282.
[19] R. Calder, G. Lewin, Reduction of stainless-steel outgassing in ultra-high vacuum, Br. J. Appl. Phys. 18 (10) (1967) 1459–1472.
[20] A.K. Riihimaki, Outgassing studies of some accelerator materials, Master's thesis, 2019, p. 63, https://cds.cern.ch/record/2679153.
[21] R. Peacock, N. Peacock, D. Hauschulz, Comparison of hot cathode and cold cathode ionization gauges, J. Vac. Sci. Technol. 9 (3) (1991) 1977–1985.
[22] D. Li, K. Jousten, Comparison of some metrological characteristics of hot and cold cathode ionisation gauges, Vacuum 70 (4) (2003) 531–541.
[23] M. Saitoh, K. Shimura, T. Iwata, T. Momose, H. Ishimaru, Influence of vacuum gauges on outgassing rate measurements, J. Vac. Sci. Technol. 11 (5) (1993) 2816–2821.
[24] A. Berman, Methods of pumping speed and gas release measurement in ionization gauge heads—A review, Vacuum 32 (8) (1982) 497–508.